

NATURAL CONVECTION WITHIN A POROUS MEDIUM CAVITY:
PREDICTING TOOLS FOR FLOW REGIME AND HEAT TRANSFER

J. L. Lage
Mechanical Engineering Department
Southern Methodist University, Dallas, TX 75275-0335, USA

(Communicated by J.P. Hartnett and W.J. Minkowycz)

ABSTRACT

A thorough analytical study is performed to identify the range of influence of each term of the general equations for flow within a fluid saturated porous medium. The first part of the analysis results into a set of algebraic equations useful in identifying the most appropriate flow regime for a given configuration (e.g. physical properties, geometry, etc.). In the second part, a unique heat transfer correlation for the general time dependent flow is obtained. This new correlation is successfully compared against theoretical and empirical results from the literature for the asymptotic flow regimes of Darcy and clean fluid, and for the Forchheimer regime. Predictions from the theoretical correlation for other (intermediate) flow regimes are also compared against numerical results available in the literature.

Introduction

The study of natural convection within a fluid saturated porous medium heated from the sides is motivated, from a practical point of view, by the broad range of applications such as in petroleum reservoir, building insulation, heat storage beds, nuclear waste repository, grain storage, and underground water contamination.

Existing flow models, from the simplest to the most complex, include the Darcy model [1], the Forchheimer-extended Darcy model [2], the Brinkman-extended Darcy model [3], and the general model [4]. The literature offers little guidance about the limitations of each model and their range of validity. This issue was stressed recently by Nield [5].

Attempts to develop a unique theoretical heat transfer correlation, valid for the

range covered by the general model, have been so far unsuccessful [6]. Theoretical heat transfer correlations found in the literature are derived from simplified flow models. For instance, Weber [7] and Bejan [8] developed heat transfer correlations using Oseen-linearization technique and Darcy model in a cavity with isothermal walls. Latter on, Bejan [9] extended the analysis for the isoflux case using the same technique. Heat transfer correlations considering Forchheimer-extended Darcy model were obtained by Poulikakos and Bejan [10] applying scale analysis and Oseen-linearization technique. The same flow model was studied also by Poulikakos [11] considering isoflux boundary conditions.

Prasad and Tuntomo [12] performed an extensive numerical study of natural convection within a vertical porous medium cavity using the Forchheimer-extended Darcy flow model. They reported two semi-empirical heat transfer correlations based upon their numerical results, one valid for Darcy regime and another for Forchheimer-extended Darcy regime.

Heat transfer correlations for Brinkman-extended Darcy model were obtained by Tong and Subramanian [13] using a Weber-type boundary layer analysis and by Lauriat and Prasad [14] based upon numerical results.

General Equations

Consider a rectangular fluid saturated porous medium cavity with impermeable surfaces. Thermophysical properties considered constant, with the saturating fluid being of Oberbeck-Boussinesq type, the general set of non-dimensional equations that governs the fluid motion within the cavity [15] is

$$\frac{\partial U}{\partial X} + \frac{\partial V}{\partial Y} = 0 \quad (1)$$

$$\phi \frac{\partial U}{\partial \tau} + \vec{V} \cdot \nabla U = - \frac{\partial P}{\partial X} + \phi J \text{Pr} \nabla^2 U - \frac{\phi^2 F}{\text{Da}} \left| \vec{V} \right| U - \frac{\phi^2 \text{Pr}}{\text{Da}} U \quad (2)$$

$$\phi \frac{\partial V}{\partial \tau} + \vec{V} \cdot \nabla V = - \frac{\partial P}{\partial Y} + \phi J \text{Pr} \nabla^2 V - \frac{\phi^2 F}{\text{Da}} \left| \vec{V} \right| V - \frac{\phi^2 \text{Pr}}{\text{Da}} V + \phi^2 \text{Ra} \text{Pr} \theta \quad (3)$$

$$\lambda \frac{\partial \theta}{\partial \tau} + \vec{V} \cdot \nabla \theta = \nabla^2 \theta \quad (4)$$

where \vec{V} is the vector velocity with horizontal, U , and vertical, V , components, and absolute value, $\left| \vec{V} \right|$, equal to $\sqrt{U^2 + V^2}$. Initial and boundary conditions, required to solve equations (1)-(4), are respectively $U = V = \theta = 0$ at $\tau = 0$, $\theta = 0.5$ at $X = 0$ and $\theta = -0.5$ at $X = L/H$, adiabatic top and bottom surfaces and no-slip surfaces.

Momentum equation (3) represents a balance among the following terms, from

left to right: transient, convective inertia, pressure, Brinkman, Forchheimer, Darcy, and buoyancy. For simplicity, but without loss of generality, the nondimensional inertia coefficient, F , is written following the model proposed by Ergun [16]:

$$F = 1.75 \left(\frac{Da}{150 \phi^3} \right)^{1/2} \quad (5)$$

The independent nondimensional parameters that govern the heat transfer and fluid flow within the cavity are then: porosity, ϕ , viscosity ratio, J , modified Prandtl number, Pr , Darcy number, Da , Rayleigh number, Ra , and volumetric specific heat ratio, λ . Also influential is the cavity aspect ratio, L/H .

Theoretical Analysis

General Flow Model

In this section, the effective ranges of various flow models quoted in the heat transfer literature are investigated by using the method of scaling. *Scale analysis*, is shown [17], for several different heat transfer phenomena, to be very effective in providing physical insight with a simplified mathematical approach.

Identifying the region within which the scaling is performed is of critical importance [18]. In the present case, the chosen scaling region extends from the hot wall (left vertical surface) towards the center of the cavity, being limited by the thickness of the upward flow layer, $\delta \leq L/2H$ (distinct layers along hot and cold walls). Scaling the Y-momentum equation, eq.(3) becomes

$$\phi \frac{V}{\tau}, V^2 \sim - \Delta P, - \phi J Pr \frac{V}{\delta^2}, - \frac{\phi^2 F}{Da} V^2, - \frac{\phi^2 Pr}{Da} V, \phi^2 Ra Pr \theta \quad (6)$$

By neglecting the vertical component of the laplacian in the scaling of the Brinkman term, it is implicitly assumed that $\delta \leq 1$. The two constraints for the flow thickness, δ , are then mutually exclusive: if $L/2H \geq 1$ then $\delta \leq 1$, otherwise $\delta \leq L/2H$.

Recognizing the correct nondimensional temperature scale within this region as $\theta \sim 0.5$, and substituting the inertia coefficient, F , leads to

$$\phi \frac{V}{\tau}, V^2 \sim - \phi J Pr \frac{V}{\delta^2}, - \frac{0.143 \phi^{1/2}}{Da^{1/2}} V^2, - \frac{\phi^2 Pr}{Da} V, \frac{\phi^2}{2} Ra Pr \quad (7)$$

In writing eq.(7), it is postulated that the pressure gradient term of eq.(3), having the same scale as the buoyancy term, can be neglected. This assumption, verified numerically [19], is used only to simplify the analysis: the more usual and laborious

approach of cross differentiating eqs.(2) and (3) in order to eliminate the pressure gradient term would lead to exactly the same scaled result.

The only term of eq.(7) that can not be neglected in any circumstance is the buoyancy term, the 'moto' of the natural convection phenomenon. The effective range of each term in eq.(7) can be determined by comparison with the buoyancy term.

Steady State Regime

For a fluid saturated porous medium with Prandtl number greater than or equal to 1, scaling the energy eq.(4) in the steady state regime gives the proper scale of δ as $V^{-1/2}$. The steady state version of eq.(7) can be written relative to the convective inertia term scale as

$$1 \sim -\phi J Pr, -\frac{0.143 \phi^{1/2}}{Da^{1/2}}, -\frac{\phi^2 Pr}{V Da}, \frac{\phi^2}{2V^2} Ra Pr \quad (8)$$

According to eq.(8), the convective inertia term becomes negligible when

$$1 \ll \frac{\phi^2}{2V^2} Ra Pr \quad (9)$$

Equation (9) is a constraint for the velocity scale, V . The V -scale depends upon the two possible flow regimes, namely Darcy regime of Forchheimer regime. For Darcy regime to be valid, from eq.(8),

$$\frac{\phi^2 Pr}{V Da} \sim \frac{\phi^2}{2V^2} Ra Pr \quad (10)$$

or, in terms of velocity,

$$V_{Da} \sim \frac{1}{2} Ra Da \quad (11)$$

Combining eqs.(11) and (9), a criterion for neglecting the convective inertia term when Darcy regime is valid can be written as

$$Da \ll 2 \phi^2 \frac{Pr}{Ra_D} \quad (12)$$

where the modified Rayleigh number, Ra_D , is defined as $(RaDa)$. This new parameter becomes increasingly important as the Darcy number is reduced. In fact, when $Da \rightarrow 0$, Ra_D becomes the only parameter to influence the solution of eqs.(1)-(4) (as demonstrated later on, the decay time of the transient regime is proportional to Darcy so the influence of the parameter λ is very limited for practical purposes).

The velocity scale of Forchheimer regime, obtained by comparing the Forchheimer term against the buoyancy term in eq.(8), is

$$V_F \sim 1.87 \phi^{3/4} (\text{Ra Pr})^{1/2} \text{Da}^{1/4} \quad (13)$$

Combining eqs.(13) and (9), the convective inertia term can be neglected in the Forchheimer regime if

$$\text{Da} \ll \frac{\phi}{49} \quad (14)$$

Equations (12) and (14) extend the scale analysis results of Lauriat and Prasad [14]. They compared the convective inertia term scale, obtained with the velocity scale of Darcy regime, against the scale of the Brinkman term. The result, valid only for Brinkman-extended Darcy flow regime, showed that the inertia term is negligible when $\phi^2 \text{Pr} \gg 1$. Noting that the porosity is a decimal number (always between 0 and 1) the convective inertia term should be negligible only for $\text{Pr} > O(10)$! One should not be too impressed by this correct result since the validity range of Brinkman-extended Darcy model is very narrow as demonstrated later on in connection with eqs.(17) and (18) for $\text{Pr} > 1$, and with eqs.(20) and (21) for $\text{Pr} \leq 1$.

The valid range of each model, Darcy or Forchheimer, can be determined by comparing the velocity scales of eqs.(11) and (13) keeping in mind the empirical evidence that the system naturally selects the smallest velocity. So, Forchheimer regime overcomes Darcy regime when the Forchheimer velocity scale, V_F , of eq.(13) becomes smaller than the Darcy velocity scale, V_{Da} , shown in eq.(11). Written in terms of Darcy number,

$$\text{Da} > 196 \phi^3 \left(\frac{\text{Pr}}{\text{Ra}_D} \right)^2 \quad (15)$$

It is worth noting that criterion (15) agrees very well with the criterion obtained in a different way by Poulikakos and Bejan [10].

The influence of the Brinkman term can be established by following the same steps used throughout the analysis of the convective inertia term. For Darcy regime, the Brinkman term scales as the buoyancy term if

$$\text{Da} \sim \frac{2}{J} \frac{\phi}{\text{Ra}_D} \quad (16)$$

For Forchheimer regime the Brinkman term scales as the buoyancy term if

$$\text{Da} \sim 0.02 \frac{1}{\phi (J \text{Pr})^2} \quad (17)$$

Equations (12), (14), (15), (16) and (17) 'map' the effective range of each flow model in a scale basis. The same procedure can be repeated for systems with Prandtl number of order 1 or smaller, by simply substituting the scale of δ in eq.(7) by [20]

$$\delta \sim \left(\frac{\text{Pr}}{V}\right)^{1/2} \tag{18}$$

The δ -scale affects only the Brinkman term so eqs.(12), (14) and (15) are valid also for $\text{Pr} < 1$. Equations (16) and (17) are replaced, respectively by

$$\text{Da} \sim 2 \frac{\phi \text{Pr}}{J \text{Ra}_D} \tag{19}$$

$$\text{Da} \sim 0.02 \frac{1}{\phi J^2} \tag{20}$$

In order to better appreciate the results presented in this section, two maps are built and shown in Fig.1 for porosity 0.4, and $J=1$. The maps locate the effective range of influence of each momentum equation term, namely convective inertia, CI, Darcy, Da, Forchheimer, F, and Brinkman, Br.

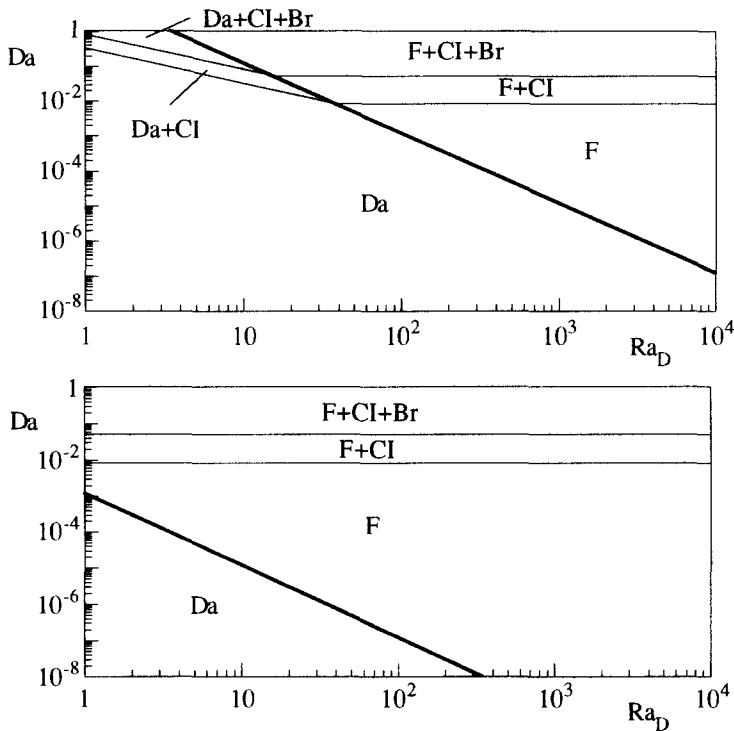


FIG. 1
 Effective range of momentum equation terms: Da - Darcy;
 F - Forchheimer; CI - convective inertia; Br - Brinkman.
 Top: $\text{Pr} = 1$; Bottom: $\text{Pr} = 0.01$

The results of Fig.1, shows, for Darcy or Forchheimer flow regimes, that the

convective inertia term, CI , is negligible if $Da < 10^{-2}$. This is true even at the low Prandtl number of 0.01. This observation confirms the conclusions of the numerical study by Manole and Lage [19].

Another important result related to Darcy regime: the convective inertia term has some effect only at very low porous modified Rayleigh numbers, $Ra_D < 65$, for $Pr = 1$. For a smaller Prandtl number, $Pr = 0.01$, its effect is negligible for the entire range of porous modified Rayleigh number, Ra_D , covered in Fig.1.

The fact that the Forchheimer term, F , becomes important before the Brinkman term, Br , when increasing Da as shown in Fig.1, agrees with the numerical results presented by Lauriat and Prasad [20]. For practical purposes, the effective range of the Brinkman term is very narrow, being limited to $Da > O(10^{-2})$.

Transient regime

During initial unsteady regime, when the velocity is very small, unsteady and buoyancy terms of eq.(7) are comparable, so

$$V \sim \frac{\tau}{2} \phi Ra Pr \quad (21)$$

Fluid motion is initiated from the quiescent state. It is reasonable then to compare the velocity scale of eq.(21) with the Darcy regime velocity scale, eq.(11). During this initial phase, the transient time decay scale is

$$\tau_{Da} \sim \frac{Da}{\phi Pr} \quad (22)$$

In most practical cases the group on the right side of eq.(22) is very small so the transient regime decays very quickly. However, eq.(22) is valid only for Darcy regime. To have a complete picture of the transient regime, it is important to consider the fact that the transient decay time scale might be long enough for the velocity scale to grow beyond the velocity scale of the Darcy regime. In this case, the velocity scale of eq.(21) must be compared with the Forchheimer velocity scale of eq.(13). The transient time decay scale, for the Forchheimer regime, then becomes

$$\tau_F \sim 3.74 \frac{Da^{3/4}}{\phi^{1/4} (Ra_D Pr)^{1/2}} \quad (23)$$

In this case, the fluid flow develops from the quiescent state to Darcy regime and then into Forchheimer regime. In order for eq.(23) to apply, the Darcy regime transient decay time has to be bigger than the Forchheimer regime decay time, $\tau_{Da} > \tau_F$,

$$Da > 196 \phi^3 \left(\frac{Pr}{Ra_D} \right)^2 \quad (24)$$

The consistency of the scale analysis for the transient regime is verified by noting that eq.(24) is exactly the same as eq.(15) that defines the transition range from Darcy to Forchheimer regime. Equations (22), (23), and (24) predict, in an order of magnitude sense, the duration of the transient regime.

Theoretical Heat Transfer Correlation

Usually, scale analysis is performed by comparing only two terms of the scaled equation at a time [17]. Considering, for natural convection flow within a fluid saturated porous medium, that one of them has to be the buoyancy term, the results are then valid only for the individual regime represented by the other term involved. In here, a scale analysis is performed keeping all terms of the scaled momentum eq.(7). The result is a general scale for fluid velocity, valid for all regimes accounted for in the general momentum equation. It is worth noting, in this new approach, the importance of preserving the signs of each scaled term.

It is wise to write eq.(7) in terms of thermal layer thickness, δ_θ , by introducing a function $A(Pr)$ that accounts for the ratio between the velocity layer thickness and the thermal layer thickness,

$$\phi \frac{V}{\tau}, V^2 \sim -\phi J Pr A(Pr) \frac{V}{\delta_\theta^2}, -\frac{0.143 \phi^{1/2}}{Da^{1/2}} V^2, -\frac{\phi^2 Pr}{Da} V, \frac{\phi^2}{2} Ra Pr \quad (25)$$

Function $A(Pr)$ is equal to 1 for $Pr \geq 1$, or equal to Pr^{-1} for $Pr < 1$ [21]. Scaling the energy equation (4), the thickness of the thermal layer scales as

$$\delta_\theta^2 \sim \frac{1}{\left(\frac{\lambda}{\tau} + V \right)} \quad (26)$$

Combining eqs.(26) and (25),

$$\phi \frac{V}{\tau}, V^2 \sim -\phi J Pr A(Pr) V \left(\frac{\lambda}{\tau} + V \right), -\frac{0.143 \phi^{1/2}}{Da^{1/2}} V^2, -\frac{\phi^2 Pr}{Da} V, \frac{\phi^2}{2} Ra Pr \quad (27)$$

Solving the quadratic equation in V presented by eq.(27) and discarding the negative root (remind that by using $\theta \sim 0.5$ we are assuming that the scale analysis is being performed within a region close to the hot wall where $V > 0$),

$$V \sim \frac{-\Pi + \left[\Pi^2 + 2\phi^2 Ra Pr \left(1 + \phi J A(Pr) Pr + \frac{0.143 \phi^{1/2}}{Da^{1/2}} \right) \right]^{1/2}}{2 \left(1 + \phi J A(Pr) Pr + \frac{0.143 \phi^{1/2}}{Da^{1/2}} \right)} \tag{28}$$

The parameter Π in eq.(28) contains the time dependent terms,

$$\Pi = \frac{\phi}{\tau} + \frac{\phi^2 Pr}{Da} + \frac{\phi J A(Pr) Pr \lambda}{\tau} \tag{29}$$

At this point, the nondimensional wall averaged heat flux transferred into the rectangular cavity is introduced as

$$Nu = \frac{q_{avg}'' L}{k_m (T_h - T_c)} = - \left(\frac{L}{H} \right) \int_0^1 \left(\frac{\partial \theta}{\partial X} \right)_{X=0 \text{ or } 1} dY \tag{30}$$

so, the Nusselt number scale at $X = 0$ is

$$Nu \sim \frac{(L/H)}{2 \delta_\theta} \tag{31}$$

The link between the general velocity scale, eq.(28), and the Nusselt scale, eq.(31), is obtained with eq.(26),

$$Nu \sim \frac{(L/H)}{2} \left(\frac{\lambda}{\tau} + V \right)^{1/2} \tag{32}$$

It is worth noting that eq.(26) assumes $\delta_\theta \leq 1$. Also, the chosen scaling region requires $\delta_\theta \leq L/2H$. These two self-exclusive constraints for δ_θ are similar to the constraints for δ analyzed in connection with eq.(6). In here, they can be used in conjunction with eq.(31) to estimate the validity range of the Nusselt number correlation in terms of the aspect ratio of the cavity. For $L/H \geq 2$, the first constraint $\delta_\theta \leq 1$ applies implying, from eq.(31), $Nu \geq L/2H \geq 1$. On the other hand, if $L/H \leq 2$ then $\delta_\theta \leq L/2H$ leading to $Nu \geq 1$. These requirements are automatically satisfied by the scale analysis performed in here due to the assumption of convective flow regime, $V > 0$, or $Nu > 1$.

A general scale for the Nusselt number is found by combining eqs.(32) and (28),

$$Nu \sim \frac{(L/H)}{2} \left\{ \frac{\lambda}{\tau} + \frac{-\Pi + \left[\Pi^2 + 2\phi^2 Ra Pr \left(1 + \phi J A(Pr) Pr + \frac{0.143 \phi^{1/2}}{Da^{1/2}} \right) \right]^{1/2}}{2 \left(1 + \phi J A(Pr) Pr + \frac{0.143 \phi^{1/2}}{Da^{1/2}} \right)} \right\}^{1/2} \tag{33}$$

Each group, on the right side of eq.(33), refers to one term of the momentum equation (3). Equation (33) provides a general correlation for the Nusselt number valid for the entire range covered by the set of general eqs.(1)-(4).

The Nusselt number scale for steady state is obtained by setting $\tau \rightarrow \infty$ in eq.(33), resulting in the following simplified correlation:

$$\text{Nu} \sim \frac{(L/H)}{2} \left\{ \frac{-\frac{\phi^2 \text{Pr}}{\text{Da}} + \left[\frac{\phi^4 \text{Pr}^2}{\text{Da}^2} + 2\phi^2 \text{Ra Pr} \left(1 + \phi J A(\text{Pr}) \text{Pr} + \frac{0.143 \phi^{1/2}}{\text{Da}^{1/2}} \right) \right]^{1/2}}{2 \left(1 + \phi J A(\text{Pr}) \text{Pr} + \frac{0.143 \phi^{1/2}}{\text{Da}^{1/2}} \right)} \right\}^{1/2} \quad (34)$$

Equation (34) indeed reduces to the correct Nusselt scale for Forchheimer regime (Nield and Bejan [6], p.24) when the groups related to Darcy, convective inertia and Brinkman terms are set equal to zero,

$$\text{Nu}_F = 0.684 \left(\frac{L}{H} \right) \phi^{3/8} \text{Da}^{1/8} (\text{Ra Pr})^{1/4} \quad (35)$$

For the clean fluid case, when the groups relating to Darcy and Forchheimer terms are set equal to zero, and $\phi = J = 1$, the Nusselt correlation reads

$$\text{Nu}_{PF} = 0.42 \left(\frac{L}{H} \right) \left(\frac{\text{Ra Pr}}{1 + A(\text{Pr}) \text{Pr}} \right)^{1/4} \quad (36)$$

Equation (36) compares well, in a scaling sense, with the result reported by Bejan [18] (pg.173) and with the Berkovsky-Polevikov correlations [22]. Also, the correlations introduced by Churchill and Chu [23], based upon experimental results for a vertical plate, are similar to eq.(36), regarding the Prandtl number effect. The last term on the right side of eq.(36) is exactly the same as the one used by Larsen and Arpaci [24] to develop an appropriate analogy between heat transfer and wall friction in natural convection from an isothermal plate within a clean fluid medium.

Figure 2 presents, for several cases, the Nusselt number obtained from eq.(34) for a square porous system with Prandtl number equal to 1. The parameter J is set as equal to 1 for simplicity. The graph shows results for two porosities, namely 0.4 (continuous line) and 0.8 (dashed line).

Although, strictly speaking, eq.(34) is not valid for the Darcy model, it predicts well the Nusselt transition between the Darcy and the Forchheimer regimes. This can be seen in Fig.2, for $\text{Da} = 10^{-2}$, the smooth transition from $\text{Nu} \sim \text{Ra}^{1/2}$, known to be valid for Darcy regime, to $\text{Nu} \sim \text{Ra}^{1/4}$, valid for Forchheimer regime (also valid

for clean fluid), as the Rayleigh number is increased. In other words, eq.(34) presents, in a continuous and smooth way, the transition between two known asymptotes, namely Darcy and Forchheimer regimes.

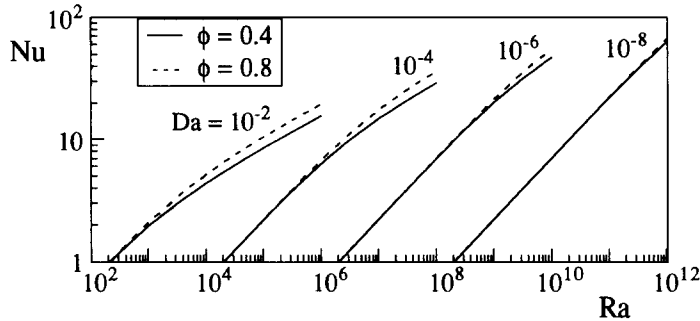


FIG. 2
Nusselt number predicted theoretically by eq. (34).

The Nusselt number predictions of Fig.2 are also compared with numerical results reported by Manole and Lage [19] showing very good agreement. Details of the numerical procedure, including grid accuracy tests, can be found in [26].

Closure

Comparing the effects of each individual term of the general momentum equation, a set of simple algebraic equations mapping the effective range of each flow model is obtained. The analysis, carried on considering the unsteady heat transfer phenomena, results into a global theoretical heat transfer correlation accounting for the effects of all terms of the momentum equation. These new tools, namely the mapping of effective range of the various flow regimes and the general heat transfer correlation, are expected to provide fundamental guidance in the field of natural convection within a fluid saturated porous medium. More important, the new scale analysis approach presented in here can be applied to different problems (e.g. isoflux boundaries, heat generation, etc.) providing a more general and complete result than the ones available in the literature.

A note about the use of general equations for modeling natural convection within a porous medium is necessary. As recently pointed out [5], there are some restriction for the applicability of general momentum equations as written in eqs.(2) and (3). In this regard, the heat transfer correlation, eq.(33), has an extra advantage: identifying the effects of each term of the momentum equation, allows individual modifications without having to perform the theoretical analysis again.

As a final note, it is suggested, for future research, comparing eq.(33) with

experimental or numerical results covering transient regime. This is specially important for large Darcy number media as anticipated by eqs.(22) and (23).

Nomenclature

A(Pr)	squared ratio of thermal and velocity layer thickness
α	thermal diffusivity, m^2/s
β	isobaric coefficient of thermal compressibility, K^{-1}
c	specific heat, $J/kg.K$
Da	Darcy number, K/H^2
δ	upward flow layer thickness
F	nondimensional inertia coefficient
ϕ	porosity
g	gravity acceleration, m/s^2
H	height of the rectangular enclosure, m
J	viscosity ratio, μ_{eff}/μ_f
k	thermal conductivity, $W/m.K$
K	permeability, m^2
L	width of the rectangular cavity, m
λ	volumetric specific heat ratio, $(\rho c)_m/(\rho c)_f$
μ	dynamic viscosity, $kg/m.s$
Nu	Nusselt number
ν	kinematic viscosity, m^2/s
p, P	pressure, Pa, $P=\phi^2 H^2(p+\rho_f g y)/(\rho_f \alpha_m^2)$
Pr	Prandtl number, ν_f/α_m
q''	heat flux, W/m^2
Ra	Rayleigh number, $g\beta H^3(T_h-T_c)/(\nu_f \alpha_m)$
ρ	density, kg/m^3
T, θ	temperature, K, $\theta=[T-(T_h+T_c)/2]/(T_h-T_c)$
t, τ	time, s, $\tau=t/(H^2/\alpha_m)$
u, v	horizontal and vertical Darcy seepage velocity components, m/s
x, y	horizontal and vertical coordinates, m
U, V	nondimensional velocity components, $(u, v)/(\alpha_m/H)$
X, Y	nondimensional coordinates, $(x, y)/H$

References

1. H. Darcy, Les Fontaines Publiques de la Ville de Dijon, Victor Dalmond, Paris, 1856.
2. P. Forchheimer, Z. Ver. D. Ing. 45, 1782 (1901).

3. H.C. Brinkman, *Appl. Sci. Res* A1, 27 (1947).
4. K. Vafai and C.L. Tien, *Int. J. Heat Mass Transfer* 24, 195 (1981).
5. D.A. Nield, *Int. J. Heat and Fluid Flow* 12, 269 (1991).
6. D.A. Nield and A. Bejan, *Convection in Porous Media*, Springer-Verlag, New York, 1992.
7. J.W. Weber, *Int. J. Heat Mass Transfer* 18, 569 (1975).
8. A. Bejan, *Lett. Heat and Mass Transfer* 6, 93 (1979).
9. A. Bejan, *Int. J. Heat and Mass Transfer* 26, 1339 (1983).
10. D. Poulikakos and A. Bejan, *Phys. Fluids* 28, 3477 (1985).
11. D. Poulikakos, *J. Heat Transfer* 107, 716 (1985).
12. V. Prasad and A. Tuntomo, *Numerical Heat Transfer* 11, 295 (1987).
13. T.W. Tong and E. Subramanian, *Int. J. Heat and Mass Transfer* 28, 563 (1985).
14. G. Lauriat and V. Prasad, *J. Heat Transfer* 109, 688 (1987).
15. C.T. Hsu and P. Cheng, *Int. J. Heat Mass Transfer* 33, 1587 (1990).
16. S. Ergun, *Chem. Engng. Prog.* 48, 89 (1952).
17. A. Bejan, *Convection Heat Transfer*, John Wiley & Sons (1984).
18. A. Bejan, *Natural Convection*, NATO Adv. Study Inst., eds. S. Kakaç, W. Aung, and R. Viskanta, 548 (1985).
19. D.M. Manole and J.L. Lage, *Int. J. Heat and Fluid Flow*, in press (1993).
20. G. Lauriat and V. Prasad, *Int. J. Heat and Mass Transfer* 32, 2135 (1989).
21. J.L. Lage, *J. Heat Transfer*, in press (1993).
22. I. Catton, *Proc. 6th Int. Heat Transfer Conf.* 6, 13 (1978).
23. S.W. Churchill and H.H. Chu, *Int. J. Heat Mass Transfer* 18, 1323 (1975).
24. P.S. Larsen and V.S. Arpaci, *Int. J. Heat Mass Transfer* 29, 342 (1986).
26. D.M. Manole and J.L. Lage, *Numerical Heat Transfer* 23, to appear (1993).

Received April 1, 1993